Chemical Physics Letters 516 (2011) 230–232

Contents lists available at SciVerse ScienceDirect

Chemical Physics Letters

journal homepage: www.elsevier.com/locate/cplett

Hydrogen-doped cubic diamond and the crystal structure of n-diamond

Bin Wen [a,b,*], Roderick Melnik [c,d], Shan Yao [b], Tingju Li [b]

[a] State Key Laboratory of Metastable Materials Science and Technology, Yanshan University, Qinhuangdao 066004, China
[b] School of Materials Science and Engineering, Dalian University of Technology, Dalian 116023, China
[c] M²NeT Lab, Wilfrid Laurier University, Waterloo, 75 University Ave. West, Ontario, Canada N2L 3C5
[d] MIT Department, University of Jyväskylä, Finland

ARTICLE INFO

Article history:
Received 22 August 2011
In final form 7 October 2011
Available online 12 October 2011

ABSTRACT

A comprehensive analysis of the crystal structure of n-diamond has been carried out based on a hydrogen-doped (H-doped) diamond model using first principles calculations. In particular, hydrogen concentration dependent elastic constants and lattice parameters for the H-doped diamond have been analyzed. Our results indicate that when the hydrogen concentration is less than 19 at.%, the H-doped diamond is mechanically stable. When the hydrogen concentration is about 4 at.%, the optimized lattice parameter, simulated XRD pattern and electronic properties for the H-doped diamond are all agree well with the corresponding experimental values of n-diamond. The results imply that the n-diamond is likely to be an H-doped diamond.

To understand the transition mechanisms and to explore new pathways to diamond, a unique procedure was designed by Hirai and Kondo in 1991, and a new possible allotrope of carbon, n-diamond, was found [1–3]. Their experimental results indicated that the lattice parameter of n-diamond is close to that of cubic ($Fd\bar{3}\,m$) diamond and many reflections in its electron diffraction pattern match that of cubic diamond except for some forbidden reflections (e.g. {200}, {222}, {420}). To date, a variety of techniques have been developed to produce the n-diamond [3,4]. In addition, n-diamond has been found on oil [5] and stratum [6,7] recently, and the list of its current and potential applications continues to grow.

Despite the successful synthesis of n-diamond using different approaches [3], the crystal structure and stability of n-diamond is still unclear. To date, all crystal structure models for n-diamond are flawed in one way or another [8–25]. For example, based on the electronic diffraction (ED) data, Jarkov et al. [23] and Konyashin et al. [24,25] suggested that the n-diamond is face-centered-cubic (FCC) with space group $Fm\bar{3}\,m$ and lattice parameter 3.57 Å. However, first principles calculations indicated that FCC carbon with lattice parameter 3.57 Å is a mechanically unstable structure [8–12]. Instead of the FCC structure, Hirai et al. [13] proposed that the n-diamond is a modified form of diamond, which is composed of hexagonal-ring-planes puckered in the opposite direction to that of cubic diamond. This model also describes a mechanically unstable structure. Recently, two crystal models of n-diamond, one named the 'glitter' model and the other one a carbon–hydrogen compound CH_x in the zincblende structure, were suggested by Bucknum [14] and Cowley [26], respectively. However, the simulated X-ray diffraction (XRD) pattern from 'glitter' models cannot reproduce the experimental patterns, and the carbon–hydrogen compound CH_x in the zincblende structure is also mechanically unstable [15–17]. Based on a catalyzed carbon black method [3], the n-diamond was studied in detail by our group [3], and two additional crystal structure models of n-diamond were suggested, one is a defective diamond model [21] and the other one is a mis-layered diamond model [22]. As it was demonstrated, these two n-diamond models are also mechanically unstable.

In most cases, the synthesis of n-diamond has been made in the presence of hydrogen [26], and the n-diamond is also a by-product of cubic diamond synthesis processing [27]. This implies that the n-diamond may be hydrogen doped (H-doped) diamond. To understand the crystal structure of n-diamond, in this Letter an H-doped diamond model has been studied using first principles calculations. Our calculated results for this model agree well with the available experimental results for n-diamond.

For our computational analysis of mechanical stability and electronic properties of H-doped diamond, we use density functional theory and the plane-wave pseudopotential technique implemented in the CASTEP package [28]. The ion–electron interaction is modeled using ultrasoft pseudopotentials [29]. The generalized gradient approximation [30] with the Perdew–Burke–Ernzerhof [31] exchange–correlation functional is used. The kinetic cutoff energy for plane waves is set to 500 eV. The $\boldsymbol{k}$ point separation in the Brillouin zone of reciprocal space is $12 \times 12 \times 12$. To describe the H-doped diamond model, a virtual crystal approximation (VCA)

* Corresponding author at: State Key Laboratory of Metastable Materials Science and Technology, Yanshan University, Qinhuangdao 066004, China.
E-mail address: wenbin@ysu.edu.cn (B. Wen).

0009-2614/$ - see front matter © 2011 Elsevier B.V. All rights reserved.
doi:10.1016/j.cplett.2011.10.014

[32] is used. The VCA is based on the creation of a virtual chemical element by mixing the pseudopotentials of the elements. For our present H-doped diamond model C_xH_{1-x}, in which carbon (C) and hydrogen (H) atoms randomly occupy a cubic diamond structure lattice, one can replace C and H by a virtual element represented by a pseudopotential operator $V_{ps} = xV_{ps}^{C} + (1-x)V_{ps}^{H}$. In this approach, the number of valence electrons to be accounted for is an average of the C and H valence electron numbers treated by each atomic pseudopotential V_{ps}^{C} and V_{ps}^{H}.

Benchmark calculations were conducted for cubic diamond. The calculated diamond C–C bond length of 0.1544 nm agrees well with the experimental values of 0.1545 nm [33]. The computed elastic constants for diamond phase are C_{11} = 1053 GPa, C_{44} = 564 GPa, and C_{12} = 119 GPa, which are in close agreement with the experimentally measured values of C_{11} = 1079 GPa, C_{44} = 578 GPa, and C_{12} = 124 GPa [34]. These results confirmed that the computational scheme utilized in this study provides a quite reasonable approximation. To verify the soundness of VCA application in H-doped diamond system, the lattice parameters and bulk module are calculated for H-doped diamond with hydrogen concentration of 3.125 at.% by using supercell method [35]. The computed lattice parameters and bulk module by supercell method are 3.577 Å and 387 GPa, which are in close agreement with the values of 3.589 Å nm and 394 GPa by using VCA method. These results further conformed that it is soundness to use VCA approximation in our present calculated system.

The hydrogen concentration dependent H-doped diamond lattice parameter and mass density are shown in Figure 1a. It is seen that with increasing hydrogen concentration, the mass density decreases while the lattice parameter increases. In the case of the H-doped diamond lattice parameter of 3.594 Å, which equals to the experimental lattice parameter of the n-diamond [18], the corresponding hydrogen concentration is 4 at.% and mass density is 3.3 g/cm^3 in H-doped diamond, respectively. This implies that the n-diamond may be an H-doped diamond with hydrogen concentration of 4 at.%. Figure 1b shows the relationship between the hydrogen concentration and elastic parameters for the H-doped diamond. It is known that the mechanical stability imposes restrictions on the elastic constants for cubic crystals, and these restrictions are [36]:

$$C_{11} > 0, C_{44} > 0, C_{11} - C_{12} > 0, C_{11} + 2C_{12} > 0. \quad (1)$$

As can be seen from Figure 1b, when the hydrogen concentration is less than 19 at.%, the H-doped diamond is mechanically stable. This means that when the hydrogen concentration is less than 19 at.%, the H-doped diamond is in a metastable phase. As seen from Figure 1c, the calculated electronic band structure implies that H-doped diamond with hydrogen concentration of 4 at.% is a conductive material, and this agrees well with the experimental results for n-diamond [3].

To study thermodynamic properties of H-doped diamond, heat of formation of H-doped diamond with respect to H_2 and diamond has been calculated by using the following equation:

$$E_{form}^{C_mH_{(1-m)}} = E_{total}^{C_mH_{(1-m)}} - mE_{diamond} - (1-m)E_{H_2}, \quad (2)$$

where $E_{total}^{C_mH_{(1-m)}}$ refers to the total energy of an $C_mH_{(1-m)}$ primitive cell that includes m C atoms and $(1-m)$ H atoms with equilibrium lattice parameters, $E_{diamond}$ is the total energy of a C atom in the pure diamond with equilibrium lattice parameters, E_{H_2} is the total

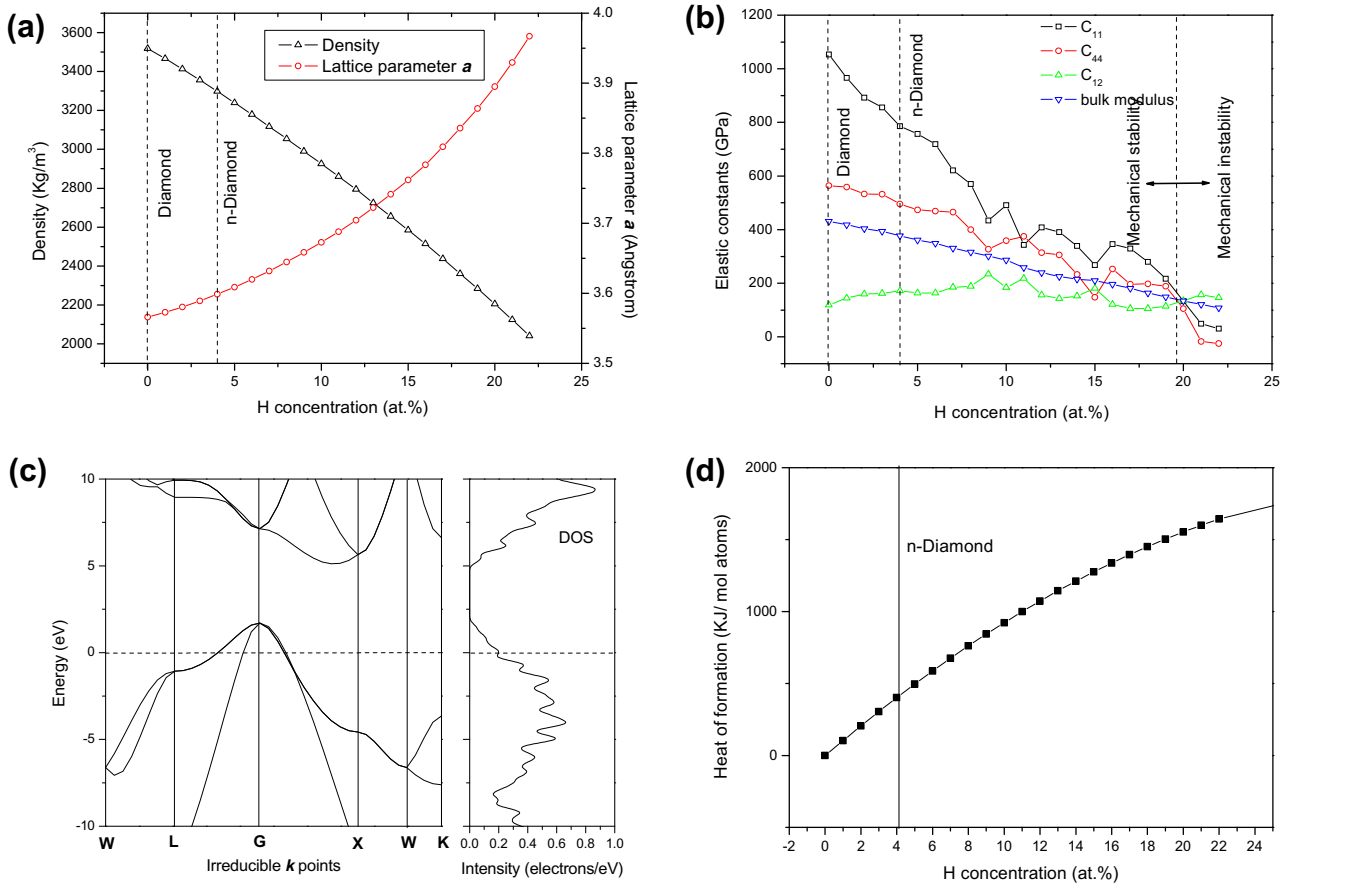

Figure 1. Hydrogen dependent H-doped diamond properties: (a) lattice parameters and mass density, (b) mechanical stability, (c) electronic band structure for H-doped diamond with hydrogen concentration of 4 at.%, and (d) heat of formation.

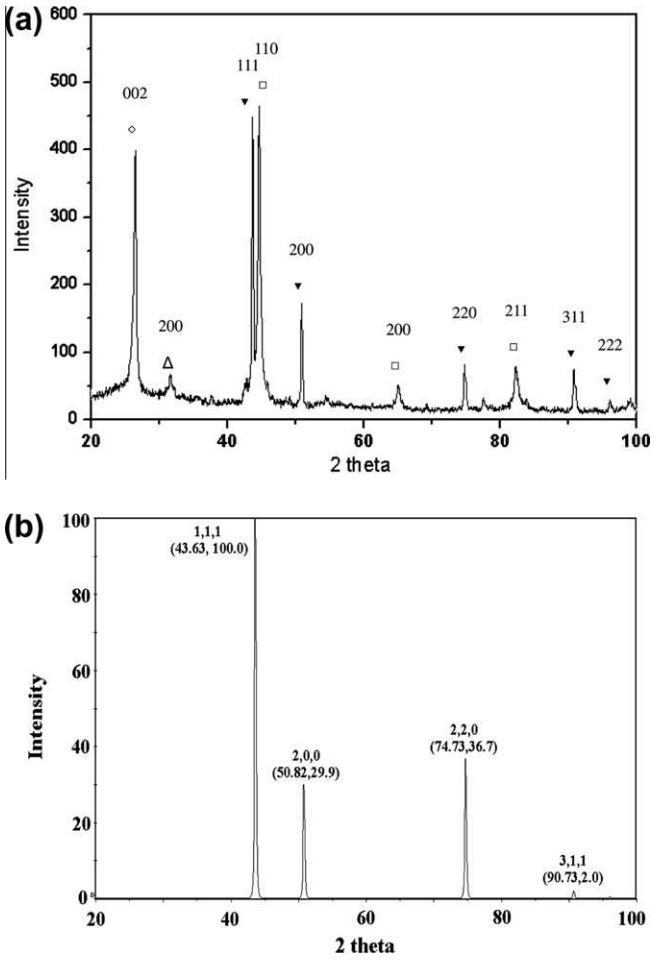

Figure 2. Comparison of (a) experimental n-diamond XRD pattern and (b) calculated XRD pattern for H-doped diamond with hydrogen concentration of 4 at.%.▼, n-Diamond; ◇, graphite; □, α-Fe; Δ, NaCl. For the experimental n-diamond pattern (a), the peaks of NaCl, α-Fe and graphite are from the catalysis and by-product of catalyzed carbon black experiment.

energy of an H atom in H_2. The calculated heat of formation for H-doped diamond is shown in Figure 1d, and as can be seen, in the hydrogen concentration range from 0 to 22 at.%, with increasing hydrogen concentration, the heat of formation increases monotonously with all the values positive. This implies that the synthesis of H-doped diamond from diamond and hydrogen is endothermic, or a high energy processing is needed.

To provide further evidence that the n-diamond structure is an H-doped diamond, XRD patterns of H-doped diamond with hydrogen concentration of 4 at.% have been simulated using a CaRIne Crystallography 3.1 program [37]. The experimental n-diamond XRD pattern [18] and the simulated XRD patterns for H-doped diamond are shown in Figure 2a and b, respectively. As shown in Figure 2a, the experimental XRD patterns not only include n-diamond peaks, but also include some other non-n-diamond peaks due to the mixed sample from catalyzed carbon black method. The detailed description of catalyzed carbon black method can be found in [18]. In brief, an admixture of the carbon black N231 powders and colloidal $Fe(OH)_3$ were compressed into an open stainless steel tank of 100 ml capacity, with a 10:1 mass ratio of carbon and iron in the mixture. The tank was first maintained at 300 °C for 100 min and sealed in air. Then it was maintained at 1100 °C for 30 min and finally cooled to room temperature in the furnace. After washing with distilled water, the n-diamond powders were dried in an oven at 110 °C. The final n-diamond powder sample was obtained. Therefore, the final n-diamond samples not only include n-diamond, but also include catalysis α-Fe, and by-product graphite etc. If we do not consider the intensity of XRD peak, the simulated XRD peak positions agree well with our previous experimental data for n-diamond [18].

In summary, an H-doped diamond model has been developed by using first principles calculations and applied to the analysis of the crystal structure of n-diamond. Our results indicated that when the hydrogen concentration is less than 19 at.%, the H-doped diamond is mechanically stable. When hydrogen concentration is about 4 at.%, the optimized lattice and simulated XRD pattern agree well with the experimental data for n-diamond. The results obtained for the electronic band structure implied that the H-doped diamond with hydrogen concentration of 4 at.% is a conductive material, and this also agrees well with the experimental results for n-diamond. Therefore, the n-diamond structure is likely to be an H-doped diamond.

Acknowledgements

This work was supported by the National Natural Science Foundation of China (Grants 50772018) and the Program for New Century Excellent Talents in Chinese Universities (NCET-07-0139). RM acknowledges the support from the NSERC and CRC program. This work was made possible by the facilities of the Shared Hierarchical Academic Research Computing Network (SHARCNET), Canada.

References

[1] H. Hirai, K.I. Kondo, Science 253 (1991) 772.
[2] B. Wen, T. Li, C. Dong, J. Jin, New Carbon Mater. 19 (2004) 319.
[3] B. Wen, J. Zhao, T. Li, Int. Mater. Rev. 8 (2007) 62 (and the references therein).
[4] B. Wang, C. Shu, C. Wang, J. Mater. Chem. 20 (2010) 7104.
[5] P. Santiago, G.A.C. Bragado, M.M. Almazo, J. Murgich, M.J. Yacaman, Energy Fuels 18 (2004) 390.
[6] D.J. Kennett et al., Science 323 (2009) 94.
[7] D.J. Kennett et al., PNAS 106 (2009) 12623.
[8] C.J. Pickard, V. Milman, B. Winkler, Diamond Relat. Mater. 10 (2001) 2225.
[9] G. Murrieta, A. Tapia, R. de Coss, Carbon 42 (2004) 771.
[10] M.T. Yin, M.L. Cohen, Phys. Rev. Lett. 50 (1983) 2006.
[11] C. Mailhiot, A.K. McMahan, Phys. Rev. B 44 (1991) 11578.
[12] J.Q. Broughton, M.J. Mehl, Phys. Rev. B 59 (1999) 9259.
[13] H. Hirai, K.I. Kondo, Appl. Phys. Lett. 64 (1992) 414.
[14] M.J. Bucnnum, I. Stamatin, E.A. Castro, Mol. Phys. 103 (2005) 20.
[15] C. Cab, G. Murrieta, G. Canto, G. Oskam, R. de Coss, Carbon 47 (2009) 1637.
[16] T. Singh, M.J. Behr, E.S. Aydil, D. Maroudas, Chem. Phys. Lett. 474 (2009) 168.
[17] M. Dadsetani, J.T. Titantah, D. Lamoen, Diamond Relat. Mater. 19 (2010) 73.
[18] B. Wen et al., J. Phys. Condens. Matter 15 (2003) 8049;
B. Wen et al., J. Phys. Condens. Matter 16 (2004) 2991;
B. Wen et al., J. Phys. Condens. Matter 16 (2004) 6891.
[19] B. Wen et al., Appl. Phys. B: Lasers Opt. 83 (2006) 629.
[20] B. Wen et al., J. Phys. D Appl. Phys. 39 (2006) 1960.
[21] B. Wen, J. Zhao, T. Li, C. Dong, J. Jin, Diamond Relat. Mater. 15 (2006) 1323.
[22] B. Wen, J. Zhao, T. Li, C. Dong, New J. Phys. 8 (2006) 62.
[23] S.M. Jarkov, Ya.N. Titarenko, G.N. Churilov, Carbon 36 (1998) 595.
[24] I. Konyashin, A. Zern, J. Mayer, F. Aldinger, V. Babaev, V. Khvostov, M. Guseva, Diamond Relat. Mater. 10 (2001) 99.
[25] I. Konyashin, V. Khvostov, V. Babaev, M. Guseva, J. Mayer, A. Sirenko, Refract. Met. Hard Mater. 24 (2006) 17.
[26] J.M. Cowley, R.C. Mani, M.K. Sunkara, M. O'Keeffe, C. Bonneau, Chem. Mater. 16 (2004) 4905.
[27] M.L. Terranova, D. Manno, M. Rossi, A. Serra, E. Filippo, S. Orlanducci, E. Tamburri, Cryst. Growth Des. 9 (2009) 1245.
[28] S.J. Clark, M.D. Segall, C.J. Pickard, P.J. Hasnip, M.I.J. Probert, K. Refson, M.C. Payne, Z. Kristallogr. 220 (2005) 567.
[29] D.R. Hamann, M. Schluter, C. Chiang, Phys. Rev. Lett. 43 (1979) 1494.
[30] M.C. Payne, M.P. Teter, D.C. Allan, T.A. Arias, J.D. Joannopoulos, Rev. Mod. Phys. 64 (1992) 1045.
[31] J.P. Perdew, K. Burke, M. Ernzerhof, Phys. Rev. Lett. 77 (1996) 3865.
[32] L. Bellaiche, D. Vanderbilt, Phys. Rev. B 61 (2000) 7877.
[33] J. Donohue, The Structures of the Elements, Wiley, New York, US, 1974.
[34] H.J. McSkimin, P. Andreatch, J. Appl. Phys. 43 (1972) 2944.
[35] P. Larson, S. Satpathy, Phys. Rev. B 79 (2009) 054502.
[36] M. Born, K. Huang, Dynamical Theory of Crystal Lattices, Clarendon Press, Oxford, UK, 1954 (Chapter III).
[37] CaRIne Crystallography 3.1 program is crystallographic software for research and teaching distributed by C. Boudias, D. Monceau.